



Heart failure with preserved ejection fraction in post myocardial infarction patients: a myocardial magnetic resonance (MR) tissue tracking study

Han Li¹, Yue Zheng¹, Xin Peng¹, Hui Liu¹, Yue Li¹, Zhaoxin Tian¹, Yang Hou², Shiqi Jin¹, Huaibi Huo¹, Ting Liu^{1^}

¹Department of Radiology, The First Hospital of China Medical University, Shenyang, China; ²Department of Radiology, Shengjing Hospital of China Medical University, Shenyang, China

Contributions: (I) Conception and design: H Li, H Huo, T Liu; (II) Administrative support: T Liu; (III) Provision of study materials or patients: T Liu; (IV) Collection and assembly of data: H Li, H Huo, Y Zheng, X Peng, H Liu, Y Li, Z Tian; (V) Data analysis and interpretation: H Li, H Huo, S Jin, Y Hou, T Liu; (VI) Manuscript writing: All authors; (VII) Final approval of manuscript: All authors.

Correspondence to: Ting Liu; Huaibi Huo. Department of Radiology, The First Hospital of China Medical University, 155 Nanjing Bei Street, Heping, Shenyang 110001, China. Email: cmuliuting@sina.cn; hhb950120@sina.com.

Background: This study aimed to explore the value of cardiac magnetic resonance tissue tracking (CMR-TT) technology in evaluating heart failure with preserved ejection fraction (HFpEF) in patients with chronic myocardial infarction (CMI).

Methods: Between June 2016 and March 2022, we included a consecutive series of 92 patients with CMI and 40 healthy controls in this retrospective study. The CMI patients enrolled were divided into different subgroups [HFpEF-CMI group (n=54) and non-heart failure (HF)-CMI group (n=38)] according to the Heart Failure Association (HFA)-PEFF (step 1: P, pre-test assessment; step 2: E, echocardiography and natriuretic peptide score; step 3: F1, functional testing; step 4: F2, final aetiology) diagnostic algorithm. CMR scan was performed at the First Hospital of China Medical University. Quantitative measurements of myocardial damage, such as myocardial strain parameters of both ventricles derived by CMR-TT and infarct size and transmural by late gadolinium enhancement (LGE), were assessed. One-way analysis of variance, independent samples *t*-test, and rank sum test were used to compare myocardial impairment among groups. Pearson or Spearman correlation coefficient was used to measure correlations between left ventricular (LV) strains and clinical and functional parameters. Logistic regression analysis and receiver operating characteristic (ROC) curve were performed to identify the best parameter for diagnosing HFpEF-CMI.

Results: HFpEF-CMI patients demonstrated significantly impaired LV strains and strain rates in all of the three directions (radial, circumferential and longitudinal) compared to non-HF-CMI patients and healthy controls ($P < 0.001$ for all), whereas only global longitudinal strain (GLS) was significantly impaired in HFpEF-CMI patients *vs.* controls for right ventricular strain parameters ($P < 0.001$). LV strains showed moderate correlation with N-terminal pro-brain natriuretic peptide (radial, circumferential and longitudinal strain, $R = -0.401$, $R = 0.408$, $R = 0.407$, respectively, $P < 0.001$ for all). LV strains in the three directions (radial, circumferential and longitudinal) [area under ROC curve (AUC) = 0.707, 95% confidence interval (CI): 0.603–0.797; AUC = 0.708, 95% CI: 0.604–0.798; AUC = 0.731, 95% CI: 0.628–0.818; respectively, $P < 0.01$ for all] were discriminators for HFpEF-CMI and non-HF-CMI. LV strains and myocardial infarction volume were independent factors in multi-logistic regression analysis after adjusting for body mass index, age, and sex ($P < 0.05$ for all).

[^] ORCID: 0000-0002-0516-6996.

Conclusions: CMR-TT provides clinicians with useful additional imaging parameters to facilitate the assessment of CMI patients with HFpEF. LV strain parameters can detect early cardiac insufficiency in patients with HFpEF-CMI and have potential value for discriminating between HFpEF and non-HF patients post-CMI.

Keywords: Heart failure with preserved ejection fraction (HFpEF); cardiac magnetic resonance tissue tracking (CMR-TT); chronic myocardial infarction (CMI); myocardial strain; late gadolinium enhancement (LGE)

Submitted Jul 28, 2022. Accepted for publication Dec 11, 2022. Published online Dec 26, 2022.

doi: 10.21037/qims-22-793

View this article at: <https://dx.doi.org/10.21037/qims-22-793>

Introduction

As a heterogeneous clinical syndrome with complex pathophysiological characteristics, heart failure (HF) is the final stage of multiple cardiovascular diseases. According to the most recent international recommendations, HF is classified as HF with reduced ejection fraction (HFrEF) [left ventricular ejection fraction (LVEF) $\leq 40\%$], HF with mid-range ejection fraction (HFmrEF) ($40\% < \text{LVEF} < 50\%$), and HF with preserved ejection fraction (HFpEF) (LVEF $\geq 50\%$) (1). HFpEF has the same adverse outcomes as HFrEF and is increasingly recognized as a significant cause of higher morbidity, mortality, and rehospitalization in patients with HF (2,3). Contrary to the increasing incidence of HFpEF, the number of clinical trials focusing on HFpEF is obviously less than on HFrEF (4). Established ischemic heart disease (IHD) is an important underlying pathogenic and prognostic factor in all types of HF (5). HFpEF with chronic myocardial infarction (HFpEF-CMI) and non-HF-CMI may display different clinical, radiological, and pathological characteristics, outcomes, and prognoses. Diagnostic techniques are needed with accurate quantitative results and better indicators for diagnosing HF patients (6).

Cardiac magnetic resonance tissue tracking (CMR-TT) is a validated tool that provides incremental information in assessing patients with HF (7) and patients with CMI (8). Additionally, studies have indicated that CMR often identifies new pathology and better establishes specific diagnoses than echocardiography in HFpEF patients (6). Therefore, we hypothesize that CMR-TT technology could detect the subtle difference in cardiac dysfunction between HFpEF-CMI patients, non-HF-CMI patients, and healthy controls and provide more effective imaging parameters for diagnosing HFpEF-CMI. We present the following article in accordance with the STARD reporting checklist (available at <https://qims.amegroups.com/article/view/10.21037/qims-22-793/rc>).

Methods

Study population

We retrospectively analyzed the CMI patients enrolled in a long-term multi-disciplinary cooperation (Department of Radiology, Ultrasound, and Cardiology) myocardial infarction (MI) study which began in June 2016. The experimental data were collected until March 2022. The inclusion criteria were: (I) patients had suffered a prior MI as defined by the Fourth Universal Definition of Myocardial Infarction (9); (II) had undergone CMR and echocardiography at 6–12 months' follow-up in the First Hospital of China Medical University. The exclusion criteria were: (I) lower CMR quality image; (II) lack of clinical data; (III) LVEF $< 50\%$. We included a consecutive series of 92 patients with CMI in this study. All patients enrolled had complete clinical data and laboratory examinations. The follow-up echocardiography and CMR scan were performed on the same day.

The CMI patients enrolled were divided into different subgroups [HFpEF-CMI group (n=54) and non-HF-CMI group (n=38)] according to clinical symptoms and the Heart Failure Association (HFA)-PEFF (step 1: P, pre-test assessment; step 2: E, echocardiography and natriuretic peptide score; step 3: F1, functional testing; step 4: F2, final aetiology) diagnostic algorithm, a consensus recommendation from the HFA of the European Society of Cardiology (ESC) (10). The inclusion criteria of HFpEF-CMI were: (I) typical HF symptoms and/or signs; (II) LVEF $\geq 50\%$; (III) at least one additional evidence below: (i) left ventricular (LV) diastolic dysfunction, (ii) left ventricular hypertrophy (LVH) and/or left atrial enlargement (LAE); (IV) a total score ≥ 5 or a score of 2–4 but confirmed to be HFpEF through invasive hemodynamic measurements. The inclusion criteria of non-HF-CMI were: (I) LVEF $\geq 50\%$; (II) having a score of 0–1 or an intermediate score (2–4 points) but confirmed to be normal through invasive hemodynamic

measurements. Eight patients in the HFpEF-CMI group and eleven in the non-HF-CMI group had an invasive hemodynamic assessment to reach the final diagnosis. Forty healthy subjects ≥ 18 years of age, without evidence of known cardiac disease in clinical symptoms, routine cardiac physical examination, electrocardiograph (ECG), and CMR examination were recruited as the control group. The study was conducted in accordance with the Declaration of Helsinki (as revised in 2013). This study was approved by the institution ethics review board of the First Hospital of China Medical University (No. KT2021213). All subjects provided written informed consent.

CMR acquisition

CMR studies were performed on 3.0T (Magnetom Verio, Siemens Medical, Erlangen, Germany). The CMR images were acquired using the protocol reported previously (8), including short-axis (SAX) balanced steady-state free precession (SSFP) cine imaging and late gadolinium enhancement (LGE). SSFP cine images were acquired with ECG gated during brief periods of breath-holding at the end of a shallow expiration in the following planes: LV 2-chamber views, 4-chamber views, and SAX planes covering the entire left ventricle from base to the apex. The scan was performed using the following parameters: Cine-SSFP: repetition time (TR) = 40.4 ms, echo time (TE) = 2.4 ms, flip angle 12° , and generalized auto-calibrating partial parallel acquisition (GRAPPA) with a parallel acceleration factor of 2. LGE: TR = 750 ms, TE = 1.6 ms, inversion time (TI) = 300 ms, flip angle 20° , and bandwidth = 465 Hz/pixel. At 8–10 minutes after bolus administration of gadolinium-diethylenetriamine penta-acetic acid (Gd-DTPA), phase-sensitive inversion recovery (PSIR) was acquired.

CMR image analysis

CMR imaging data were analyzed by two radiologists with more than 6 years of diagnostic experience without knowing other measurements and clinical information. If there was disagreement, the senior radiologists adjudicated. The acquired magnetic resonance (MR) images were processed on CVI42 (Version 5.3.4, Circle Cardiovascular Imaging, Canada). CMR-TT algorithms were performed on the cine sequence, including the SAX and three long-axis (LAX) views (2-, 3-, and 4-chamber). The SAX views comprised a stack of contiguous SAX slices covering the entire LV and right ventricular (RV) from base to apex, excluding slices

that included the outflow tract or the mitral valve planes. The endocardium and epicardium were automatically detected on cine images in the end-diastolic and end-systolic phases at each SAX and LAX level. The trabecula was excluded from the endocardial contour. Contours were manually adjusted by the observer for accurate tracking if required. The movement of tissue voxels in the plane throughout the cardiac cycle (25 frames/cardiac cycle) was then automatically tracked by the software to quantify the movement of the RV free-wall and LV entire myocardium (free-wall + septum). Longitudinal strain parameters were calculated from images of 2-, 3- and 4-chamber cine sequences. Circumferential and radial strain parameters were calculated on SAX Cine CMR covering the whole heart. The myocardial strain was defined as the percentage of myocardial fiber shortening at the end of contraction versus the end of diastole. Myocardial strain rate is defined as the changes in myocardial strain over time. The observer manually identified systolic, early, and late diastolic peaks from each strain rate curve derived from the software. The peak early diastolic strain rate (PEDSR) and peak late diastolic strain rate (PLDSR) were defined as the first and second peaks in strain rate seen in diastole, with the second peak coinciding with atrial contraction (Figure S1) (11). The global peak strain, peak systolic strain rate (PSSR), and diastolic strain rate (including PEDSR and PLDSR) in the three directions of both ventricles were obtained. Infarct size and transmuralities were analyzed on the LGE sequence. According to the 2002 American Heart Association, 17 segments were obtained. The infarct segment and corresponding distal normal segment were identified from 17 segment images. MI was identified on LGE images and quantified at a threshold of mean + 5 standard deviation (SD) intensity of the distal myocardium. Infarct transmuralities were calculated from data provided by the software. It was determined along 100 equally spaced chords on each slice as percentage of infarct area. Averaging the infarct of all chords with $\geq 1\%$ scar extent, we would acquire the mean transmuralities rate. Examples of measurements in Cine and LGE are shown in Figure 1.

Data reproducibility

The intra-observer variability of TT-derived strain parameters was assessed by intragroup correlation coefficient (ICC) in 20 randomly selected patients from the three groups, with a time interval of 2 weeks between analyses. The interobserver reliability was assessed in

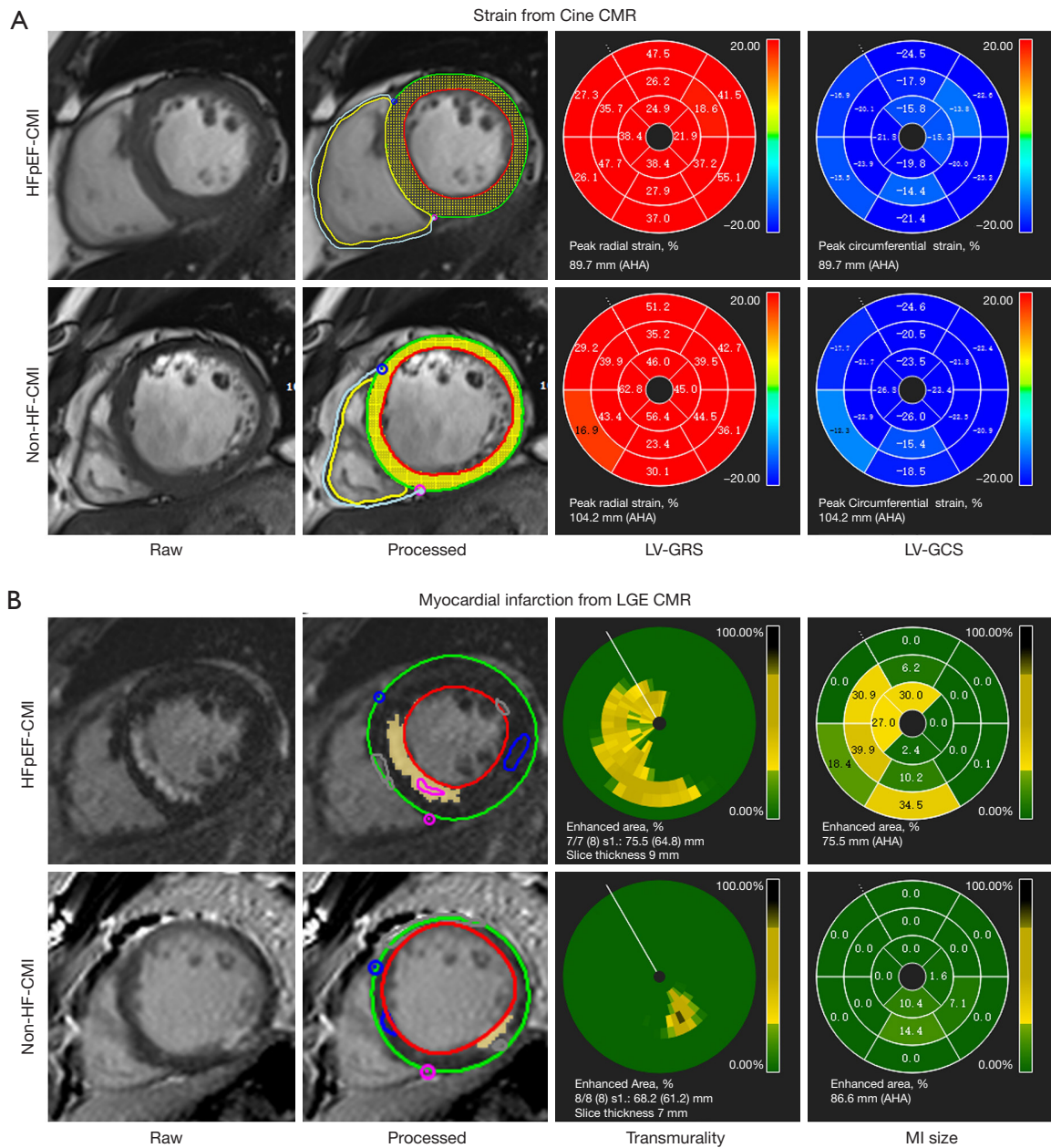


Figure 1 Imaging analysis procedure at CVI42 of a patient with HFpEF-CMI (male, 61 years old) and a patient with non-HF-CMI (male, 53 years old). (A) Strain analysis at CMR by using tissue tracking was performed on short-axis views; (B) Transmurality and MI size analysis by using LGE was performed on short-axis views. AHA, American Heart Association; HFpEF, heart failure with preserved ejection fraction; CMI, chronic myocardial infarction; HF, heart failure; LV, left ventricular; GRS, global radial strain; GCS, global circumferential strain; LGE, late gadolinium enhancement; MI, myocardial infarction; CMR, cardiac magnetic resonance.

the same 20 patients by comparing the results from two professional and independent observers (H Li and H Huo) without knowing other results and clinical information.

Statistical analysis

Statistical analyses were performed using SPSS Statistics (version 25, IBM, Armonk, NY, USA), MedCalc Statistical

Software (version 19.6.4 MedCalc Software Ltd.; Ostend, Belgium), and the “PredictABEL” package in R software (version 3.6.3; R Foundation, Vienna, Austria). Measurement data were expressed as mean \pm SD, and count data were expressed as median (interquartile range) or counts (percentages). One-way analysis of variance (ANOVA), independent samples *t*-test, rank sum test, Chi-square test, and Fisher’s exact test were used to assess variables among the groups according to different types of data. Pearson or Spearman correlation coefficient was used to measure correlations between strain parameters and clinical and functional parameters. A receiver operating characteristic (ROC) curve and pairwise comparisons of ROC curves were performed to identify the best parameter or model for diagnosing HFpEF-CMI. Logistic regression was performed to determine independent contributors of HFpEF-CMI versus non-HF-CMI. Three multivariable logistic regression models for diagnosing HFpEF-CMI were created manually, selecting the clinical variables [age, sex, and body mass index (BMI)] and CMR marker (MI sizes) combined with one of the LV strains in three directions. The comparisons of models were performed with the R software by calculating the net reclassification index (NRI). A *P* value <0.05 was used to determine statistical significance.

Sample size calculation

The sample size of the current study was calculated using the Power Analysis and Sample Size Software (PASS.15.0.5, NCSS, LLC. Kaysville, Utah) according to the tests for one ROC curve (12,13). The statistical power was set as 0.90, and the $\alpha=0.05$. We assumed that the numbers of HFpEF patients and non-HF patients were equal ($N_+ = N_-$). The one-sided test was used. The null hypothesis was that AUC_0 [area under the ROC curve (AUC), H_0] = 0.50. The alternative hypothesis was that AUC_1 (H_1) = 0.70, which was determined by the diagnostic accuracy of strain parameters reported in previous literatures (14,15). Finally, PASS software indicated that the minimum sample size should be 33 cases in each group.

Results

Baseline characteristics and anthropometric variables

A total of 132 subjects who underwent CMR were included in this study, including 92 CMI patients (average age, 59.1 ± 11.0 years; range, 34–89 years; 88.0% male) and 40 healthy controls (average age, 55.5 ± 8.6 years; range,

39–71 years; 62.5% male). According to the ESC guidelines (2), 54 HFpEF-CMI patients (58.7%) and 38 non-HF-CMI patients (41.3%) were divided into two subgroups. The flowchart of the study population is shown in *Figure 2*. The baseline clinical characteristics of subjects are summarized in *Table 1*. Patients with HFpEF-CMI and non-HF-CMI were older than the healthy controls ($P < 0.01$ for all). There were more male patients in the HFpEF-CMI group (85.2% male) and the non-HF-CMI group (92.1% male) than the control group ($P < 0.01$ for all). Patients with HFpEF-CMI ($P < 0.01$) and non-HF-CMI ($P < 0.001$) had a higher BMI than the control subjects. There was no significant difference in heart rate and hemoglobin among the groups. HFpEF-CMI patients had a higher level of N-terminal pro-brain natriuretic peptide (NT-proBNP) than non-HF-CMI [414.80 (271.40 – 977.90) *vs.* 55.74 (34.07 – 105.75) pg/mL, $P < 0.001$]. No significant differences were found between the two subgroups in smoking, alcohol drinking history, and the incidence of hypertension, diabetes mellitus, and hyperlipidemia. A trend toward a more frequent use of loop diuretics was noted in HFpEF-CMI patients.

Basic cardiac function parameters

The basic cardiac function parameters derived from CMR and transthoracic echocardiography (TTE) are presented in *Table 2*. The control group has a significantly lower left ventricular end-diastole volume index (LVEDVi) than HFpEF-CMI patients and non-HF-CMI patients ($P < 0.001$ for all). The right ventricular ejection fraction (RVEF) in non-HF-CMI patients was significantly lower than in the control group ($P < 0.05$). There was no significant difference in the right ventricular end-diastole volume index (RVEDVi) among the three groups. HFpEF-CMI patients had significantly larger MI sizes than non-HF-CMI patients ($13.5\% \pm 9.4\%$ *vs.* $9.6\% \pm 6.6\%$, $P < 0.05$). Additionally, HFpEF-CMI patients had significantly higher LV mass index (LVMI) ($P < 0.001$) and left atrial volume index (LAVI) ($P < 0.05$) than non-HF-CMI patients. Comparison among HFpEF-CMI, non-HF-CMI, and controls regarding the echocardiographic finding showed that HFpEF-CMI patients and non-HF-CMI patients had significantly lower LVEF than healthy controls ($P < 0.001$ for all). There was a significant difference in the LA dimension ($P < 0.05$) but no significant difference in E/e' ratio (the ratio of mitral peak velocity of the early filling to mean early diastolic mitral annular velocity), e' septal velocity, and e' lateral velocity between patients with HFpEF-CMI and non-HF-CMI.

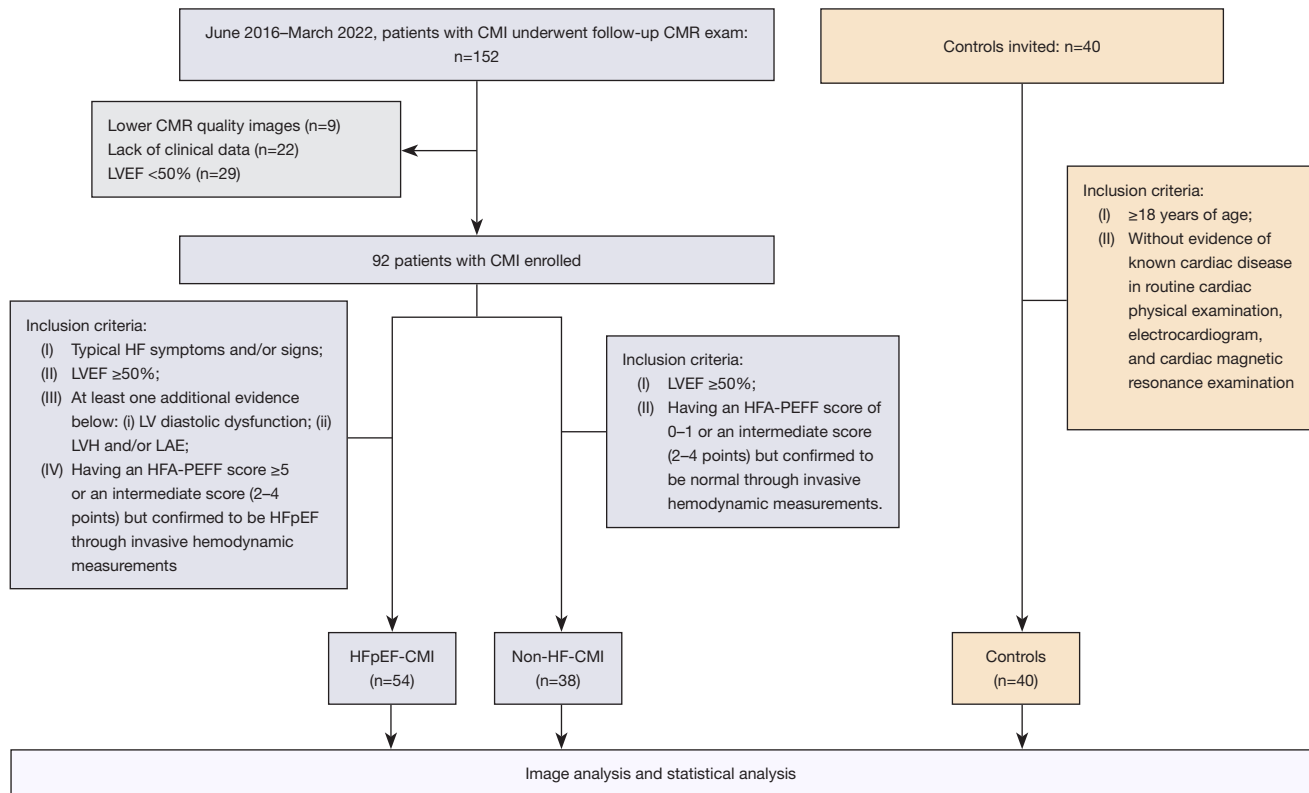


Figure 2 Patient flowchart. The flowchart shows the involvement of patients and controls. CMI, chronic myocardial infarction; CMR, cardiac magnetic resonance, HF, heart failure; HFpEF, HF with preserved ejection fraction; LVEF, left ventricular ejection fraction; LVH, left ventricular hypertrophy; LAE, left atrial enlargement; HFA, Heart Failure Association; PEFF, step 1: P, pre-test assessment; step 2: E, echocardiography and natriuretic peptide score; step 3: F1, functional testing; step 4: F2, final aetiology.

LV strains and strain rates

LV strains and strain rates quantified by cine CMR are summarized in *Table 3* and *Figure 3*. The absolute values of LV strains and strain rates, including global radial strain (GRS), global circumferential strain (GCS), global longitudinal strain (GLS), and PSSR in three directions were all significantly reduced in the HFpEF-CMI group as compared with the non-HF-CMI group, and in two test subgroups as compared with the control group ($P < 0.01$ for all). Compared to non-HF-CMI patients, HFpEF-CMI patients showed significantly reduced deformation in radial PEDSR, circumferential PEDSR, and longitudinal PLDSR ($P < 0.05$ for all).

RV strains and strain rates

Group comparisons of RV strains and strain rates are listed in *Table 4* and *Figure 3*. There were few statistically significant differences among the groups in the RV strain

values except GCS, GLS, and longitudinal PLDSR. Non-HF-CMI patients had a lower absolute value of RV-GCS than healthy controls ($P < 0.01$). Two test subgroups had a lower absolute value of RV-GLS than healthy controls ($P < 0.001$ for all). The HFpEF-CMI patients had a higher longitudinal PLDSR than non-HF-CMI patients ($P < 0.05$).

Correlation of strain parameters with CMR variables and laboratory markers

To evaluate the correlations between strain parameters and other CMR variables, and NT-proBNP, a related laboratory index, Pearson or Spearman correlation coefficient was applied. The results are shown in *Figure 4*. Among all groups, there were significant correlations between LVEF and LV strain parameters (GRS: $R = 0.468$, GCS: $R = -0.469$, GLS: $R = -0.314$, $P < 0.01$ for all). The LV strain parameters were weakly correlated with MI sizes (GRS: $R = -0.381$, GCS: $R = 0.393$, GLS: $R = 0.264$, $P < 0.05$ for all). The NT-proBNP

Table 1 Baseline clinical characteristics

Characteristics	HFpEF-CMI patients (n=54)	Non-HF-CMI patients (n=38)	Controls (n=40)	P
Age (years)	60.6±11.7 [‡]	57.0±9.6 [‡]	55.5±8.6	0.045
Male sex, n (%)	46 (85.2) [‡]	35 (92.1) [‡]	25 (62.5)	0.002
Body mass index (kg/m ²)	23.60 (21.49–25.69) [†]	25.99 (23.31–27.94) [†]	23.30 (21.60–24.55)	<0.001
Heart rate (bpm)	66.00 (59.75–73.00)	68.00 (62.75–74.75)	67.50 (59.25–75.00)	0.572
NT-proBNP (pg/mL)	414.80 (271.40–977.90)	55.74 (34.07–105.75)	–	<0.001
Hemoglobin (g/L)	120.7±27.0	124.8±26.0	–	0.588
HF symptoms, n (%)	54 (100.0)	13 (34.2)	–	<0.001
Smoking habits, n (%)	27 (50.0)	24 (63.2)	–	0.211
Alcohol drinking habits, n (%)	23 (42.6)	11 (28.9)	–	0.182
Hypertension, n (%)	35 (64.8)	21 (55.3)	–	0.355
Diabetes mellitus, n (%)	35 (64.8)	17 (44.7)	–	0.056
Hyperlipidemia, n (%)	26 (48.1)	15 (39.5)	–	0.410
Medications, n (%)				
Aspirin	39 (72.2)	34 (89.5)	–	0.044
ACEI/ARB	22 (40.7)	11 (28.9)	–	0.246
Beta-blocker	45 (83.3)	34 (89.5)	–	0.405
Statin	43 (79.6)	36 (94.7)	–	0.041
Loop diuretics	22 (40.7)	4 (10.5)	–	0.002
Clopidogrel	15 (27.8)	16 (42.1)	–	0.152

Values are mean ± standard deviation, n (%), or median (interquartile range). [†], P<0.05 vs. non-HF-CMI patients; [‡], P<0.05 vs. controls. HFpEF, heart failure with preserved ejection fraction; HF, heart failure; CMI, chronic myocardial infarction; NT-proBNP, N-terminal pro-brain natriuretic peptide; ACEI, angiotensin-converting enzyme inhibitor; ARB, angiotensin receptor blocker.

was moderately correlated with LV strain parameters (GRS: R=−0.401, GCS: R=0.408, GLS: R=0.407, P<0.001 for all). Furthermore, there is no significant correlation between transmural strain and LV strain parameters, and RV strain parameters showed no significant correlation with any other parameters.

ROC curve analysis of LV and RV parameters for differentiating HFpEF-CMI from non-HF-CMI group

ROC curves reflect the diagnostic performance of TT-derived biventricular strain parameters in identifying HFpEF-HF and non-HF-CMI (Figure 5). Among the strain parameters, LV-GRS [area under the ROC curve (AUC) =0.707, 95% confidence interval (CI): 0.603–0.797; P=0.001], LV-GCS (AUC =0.708, 95% CI: 0.604–0.798; P=0.001), and LV-GLS (AUC =0.731, 95% CI: 0.628–0.818;

P<0.001) were good discriminators for HFpEF-CMI and non-HF-CMI. The ROC curve of LV-GLS showed the largest AUC, lowest sensitivity value, and highest specificity value among the strain parameters. However, there was no statistically significant difference found in the pairwise comparison of ROC curves except for LV-GLS vs. RV-GLS (AUC =0.731, 95% CI: 0.628–0.818 vs. AUC =0.566, 95% CI: 0.458–0.669; P=0.032) (Table S1). The optimal cutoff value for LV-GRS was 24.4% (sensitivity, 63.0%; specificity, 84.2%), for LV-GCS was −15.2% (sensitivity, 61.1%; specificity, 84.2%), and for LV-GLS was −11.5% (sensitivity, 48.1%; specificity, 92.1%).

Logistic regression analysis for the association of CMR makers with HFpEF-CMI

We enrolled the parameters which showed significant

Table 2 Basic cardiac function parameters of CMR and TTE

Characteristics	HFpEF-CMI patients (n=54)	Non-HF-CMI patients (n=38)	Controls (n=40)	P
CMR parameters				
LVEDVi (mL/m ²)	72.55 (59.53–84.77) [†]	67.20 (56.74–75.44) [†]	54.02 (49.78–54.02)	<0.001
RVEF (%)	47.0±11.1	43.6±9.0 [†]	48.9±7.2	0.046
RVEDVi (mL/m ²)	57.1±14.6	61.0±12.1	59.1±12.3	0.375
MI volume (%LV)	13.5±9.4	9.6±6.6	–	0.028
Transmurality (%)	39.24 (31.46–49.83)	38.21 (27.86–46.06)	–	0.430
LV mass index (g/m ²)	63.90 (51.44–73.18)	50.37 (43.03–61.33)	–	<0.001
LA volume index (mL/m ²)	42.6±12.2	38.3±7.9	–	0.044
Echocardiography parameters				
LVEF (%)	57.9±4.8 [†]	59.0±5.6 [†]	64.0±4.9	<0.001
LA anteroposterior diameter (mm)	39.9±5.2	36.8±5.2	–	0.017
E/e' ratio	9.4 (7.9–12.7)	10.0 (8.9–11.5)	–	0.668
e' septal (cm/s)	5.4±1.5	5.7±1.2	–	0.404
e' lateral (cm/s)	8.7±2.0	9.2±2.0	–	0.451

Values are mean ± standard deviation, n (%), or median (interquartile range). [†], P<0.05 vs. controls. HFpEF, heart failure with preserved ejection fraction; HF, heart failure; CMI, chronic myocardial infarction; CMR, cardiac magnetic resonance; TTE, transthoracic echocardiography; LVEDVi, left ventricular end-diastole volume index; RVEF, right ventricular ejection fraction; RVEDVi, right ventricular end-diastole volume index; MI, myocardial infarction; LV, left ventricular; LA, left atrial; LVEF, left ventricular ejection fraction; E, the mitral peak velocity of the early filling; e', early diastolic mitral annular velocity; E/e', the ratio of E to mean early diastolic mitral annular velocity.

Table 3 CMR-TT derived LV strains and strain rates

Variables	HFpEF-CMI patients (n=54)	Non-HF-CMI patients (n=38)	Controls (n=40)	F	P
GRS, %	22.67±9.04 ^{††}	28.07±5.83 [†]	42.99±10.34	64.549	<0.001
GCS, %	-14.18±4.12 ^{††}	-16.87±2.54 [†]	-21.39±2.93	52.582	<0.001
GLS, %	-12.17 (-14.34 to -9.84) ^{††}	-14.61 (-16.01 to -12.62) [†]	-18.76 (-20.75 to -17.22)	–	<0.001
Radial PSSR, s ⁻¹	1.05 (0.77–1.43) ^{††}	1.27 (1.14–1.56) [†]	2.15 (1.77–2.56)	–	<0.001
Circumferential PSSR, s ⁻¹	-0.69 (-0.8 to -0.55) ^{††}	-0.83 (-0.94 to -0.70) [†]	-1.05 (-1.26 to -0.91)	–	<0.001
Longitudinal PSSR, s ⁻¹	-0.63 (-0.78 to -0.50) ^{††}	-0.73 (-0.84 to -0.63) [†]	-1.02 (-1.16 to -0.90)	–	<0.001
Radial PEDSR, s ⁻¹	-1.08±0.62	-1.33±0.51	–	–	0.041
Radial PLDSR, s ⁻¹	-0.62 (-0.81 to -0.44)	-0.63 (-0.99 to -0.48)	–	–	0.407
Radial PEDSR/PLDSR	1.68±1.22	2.05±0.83	–	–	0.104
Circumferential PEDSR, s ⁻¹	0.57±0.25	0.66±0.17	–	–	0.041
Circumferential PLDSR, s ⁻¹	0.53±0.21	0.56±0.17	–	–	0.475
Circumferential PEDSR/PLDSR	1.11 (0.71–1.51)	1.25 (1.01–1.51)	–	–	0.247
Longitudinal PEDSR, s ⁻¹	0.50±0.21	0.57±0.14	–	–	0.074
Longitudinal PLDSR, s ⁻¹	0.53 (0.44–0.66)	0.62 (0.56–0.75)	–	–	0.001
Longitudinal PEDSR/PLDSR	0.90 (0.64–1.22)	0.89 (0.71–1.02)	–	–	0.631

Values are mean ± standard deviation or median (interquartile range). [†], P<0.05 vs. non-HF-CMI patients; ^{††}, P<0.05 vs. controls. CMR, cardiac magnetic resonance; TT, tissue tracking; LV, left ventricular; HFpEF, heart failure with preserved ejection fraction; HF, heart failure; CMI, chronic myocardial infarction; GRS, global radial strain; GCS, global circumferential strain; GLS, global longitudinal strain; PSSR, peak systolic strain rate; PEDSR, peak early diastolic strain rate; PLDSR, peak late diastolic strain rate.

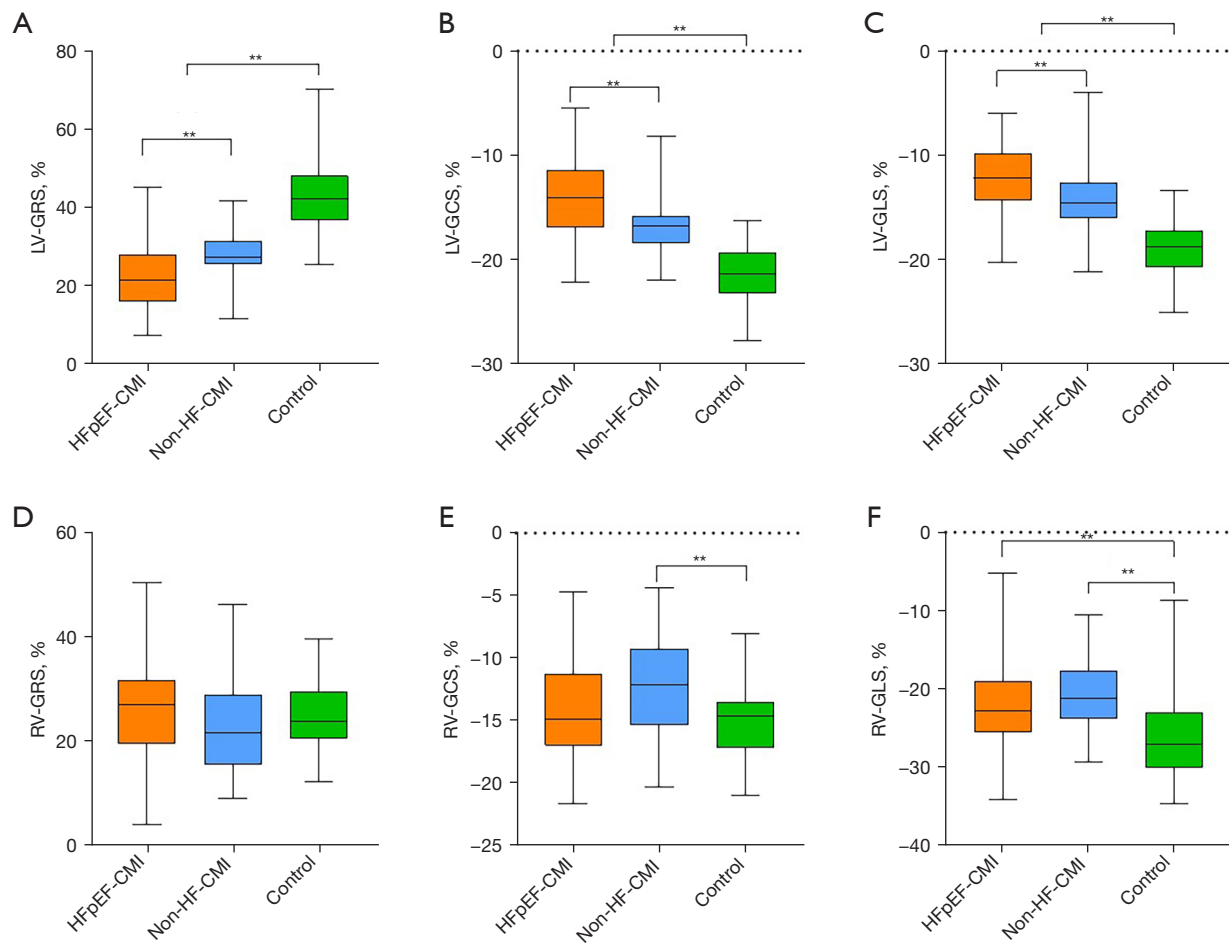


Figure 3 Comparison of strain parameters among HFpEF-CMI, non-HF-CMI, and control subjects. Boxplot of strain parameters in HFpEF-CMI, non-HF-CMI, and control subjects. (A) LV-GRS; (B) LV-GCS; (C) LV-GLS; (D) RV-GRS; (E) RV-GCS; (F) RV-GLS. **, statistically significant difference, $P < 0.01$. LV, left ventricular; RV, right ventricular; GRS, global radial strain; GCS, global circumferential strain; GLS, global longitudinal strain; HFpEF, heart failure with preserved ejection fraction; HF, heart failure; CMI, chronic myocardial infarction.

differences between the HFpEF-CMI group and the non-HF-CMI group into univariate analyses, parameters used in HFA-PEFF diagnostic algorithm were excluded. LV strain parameters were converted to categorical variables according to the cutoff values. In the univariate logistic regression analysis, all variables were significantly associated with the diagnosis of HFpEF-CMI, including $\text{BMI} \geq 25 \text{ kg/m}^2$, $\text{MI volume} \geq 9.3\% \text{ LV}$, $\text{LV-GRS} \leq 24.4\%$, $\text{LV-GCS} \geq -15.2\%$, $\text{LV-GLS} \geq -11.5\%$ (Table 5). The result of multilogistic stepwise regression analysis with these significant variables and adjustment for confounding factors (age and sex) are shown in Figure 6. In three multivariable models, LV strains and $\text{MI volume} \geq 9.3\% \text{ LV}$ were independently

significantly associated with the diagnosis of HFpEF-CMI with adjustment for age, sex, and BMI ($P < 0.05$ for all). However, there was no significant difference between these models (Table S2).

Data reproducibility

Global LV and RV strains were reproducible at the intra- and interobserver levels. The ICC for the strain parameters was summarized in Table 6. For intra- and interobserver reliability, all strain parameters showed good ICC (> 0.75). RV-GRS was the least reproducible global measurement for intraobserver reliability (ICC = 0.767). RV-GCS was the

Table 4 CMR-TT derived RV strains and strain rates

Variables	HFpEF-CMI patients (n=54)	Non-HF-CMI patients (n=38)	Controls (n=40)	F	P
GRS, %	27.15 (19.54–31.70)	21.57 (15.51–28.98)	23.80 (20.59–29.58)	–	0.076
GCS, %	–14.06±3.82	–12.36±4.30 [‡]	–15.47±2.96	6.76	0.002
GLS, %	–22.87 (–25.61 to –19.04) [‡]	–21.27 (–23.89 to –17.80) [‡]	–27.21 (–30.08 to –23.18)	–	<0.001
Radial PSSR, s ^{–1}	1.32 (1.03–1.70)	1.20 (0.88–1.50)	1.30 (1.04–1.62)	–	0.208
Circumferential PSSR, s ^{–1}	–0.75 (–0.94 to –0.59)	–0.74 (–0.96 to –0.60)	–0.84 (–1.01 to –0.68)	–	0.194
Longitudinal PSSR, s ^{–1}	–1.29 (–1.60 to –1.04)	–1.34 (–1.87 to –1.13)	–1.43 (–1.96 to –1.14)	–	0.409
Radial PEDSR, s ^{–1}	–1.06 (–1.36 to –0.80)	–1.10 (–1.31 to –0.75)	–	–	0.994
Radial PLDSR, s ^{–1}	–0.72±0.36	–0.60±0.31	–	–	0.107
Radial PEDSR/PLDSR	1.60 (0.98–2.60)	1.93 (1.40–3.04)	–	–	0.091
Circumferential PEDSR, s ^{–1}	0.53±0.20	0.59±0.25	–	–	0.224
Circumferential PLDSR, s ^{–1}	0.51±0.25	0.46±0.19	–	–	0.230
Circumferential PEDSR/PLDSR	1.07 (0.76–1.82)	1.33 (0.95–1.77)	–	–	0.236
Longitudinal PEDSR, s ^{–1}	0.93 (0.59–1.22)	0.74 (0.57–1.11)	–	–	0.292
Longitudinal PLDSR, s ^{–1}	1.27 (1.08–1.57)	1.05 (0.75–1.33)	–	–	0.008
Longitudinal PEDSR/PLDSR	0.58 (0.47–0.89)	0.74 (0.47–1.12)	–	–	0.233

Values are mean ± standard deviation or median (interquartile range). [‡], P<0.05 vs. controls. CMR, cardiac magnetic resonance; TT, tissue tracking; RV, right ventricular; HFpEF, heart failure with preserved ejection fraction; HF, heart failure; CMI, chronic myocardial infarction; GRS, global radial strain; GCS, global circumferential strain; GLS, global longitudinal strain; PSSR, peak systolic strain rate; PEDSR, peak early diastolic strain rate; PLDSR, peak late diastolic strain rate.

least reproducible global measurement for interobserver reliability (ICC =0.759).

Discussion

The principal findings are as follows: (I) TT-derived LV strain parameters demonstrated significantly intramyocardial impaired deformation in HFpEF-CMI compared to non-HF-CMI and controls in three directions; (II) compared to healthy controls, only GLS was significantly impaired in two test subgroups among RV strain parameters; (III) LV strain parameters were significantly correlated with LVEF, NT-proBNP, and MI sizes. (IV) LV strain parameters were good discriminators of HFpEF-CMI from non-HF-CMI, and the reduction of LV-GRS, GCS, and GLS remain independent diagnostic markers after adjusting BMI, age, and sex.

We retrospectively studied a cohort of participants with HFpEF and non-HF post-CMI and performed assessments of LV mechanics using CMR-TT techniques. As an aging population and effective treatment of acute coronary

syndrome resulting in reduced myocardial impairment and remodeling, the impact of IHD on HF and its subtypes is evolving. This was further underscored by a study detecting the trend of HF post-IHD events, increasingly favoring HFmrEF and HFpEF compared with HFfrEF (16). In HFpEF, series studies have demonstrated worse survival among patients with IHD than those without, as myocardial ischemia causes both diastolic and systolic dysfunction. Moreover, patients with new IHD events were more likely to transition to a lower EF category over time (5,17,18).

HFpEF-CMI patients were clinically considered to have recovered cardiac function, but the cardiac reserve and pumping capacity were significantly reduced compared with the non-HF-CMI group and control group. Despite being defined as diastolic dysfunction and preserved ejection fraction, HFpEF is characterized by mild systolic dysfunction and significant limitations in systolic reserve capacity (19). The strain and strain rate of HFpEF-CMI and non-HF-CMI patients was gradually decreased and significantly lower than that of healthy controls. HFpEF patients with IHD had a higher risk of changing to HF

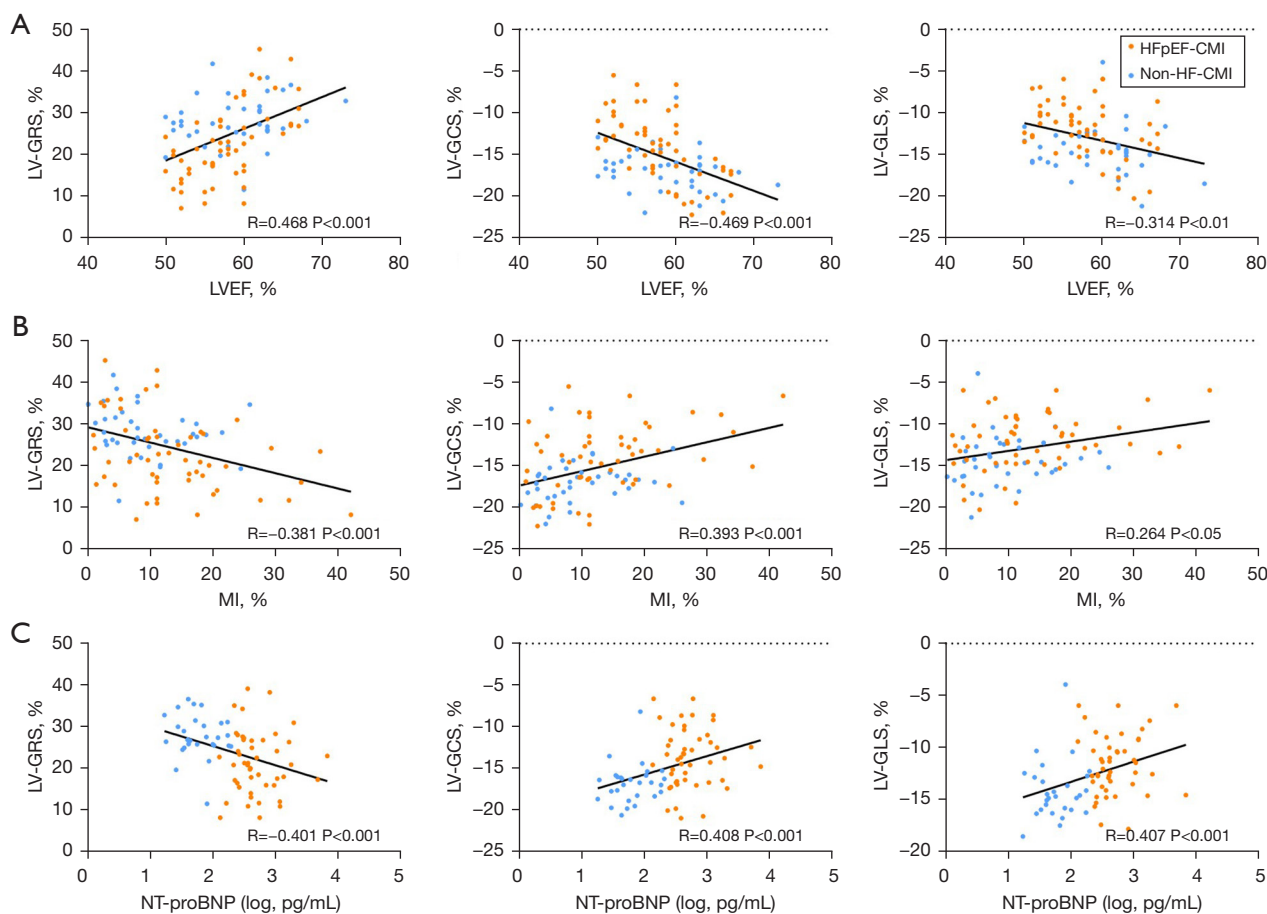


Figure 4 Correlation of strain parameters with other CMR variables and laboratory markers. Scatter plot between CMR variables and laboratory markers. (A) LV strain parameters and LVEF; (B) LV strain parameters and MI; (C) LV strain parameters and NT-proBNP. LVEF, left ventricular ejection fraction; NT-proBNP, N-terminal pro-brain natriuretic peptide, MI, myocardial infarction; LV, left ventricular; GRS, global radial strain; GCS, global circumferential strain; GLS, global longitudinal strain; CMR, cardiac magnetic resonance; HFpEF, heart failure with preserved ejection fraction; CMI, chronic myocardial infarction.

phenotypes with lower EF (5). In the past decades, previous studies have also highlighted that the clinical symptoms of HFpEF are not caused by diastolic dysfunction only. There are many hypotheses regarding the potential pathophysiology of HFpEF, including the damage of systolic reserve capacity and heart rate reserve (19,20), myocardial fibrosis and ventricular remodeling (21-23), atrial dysfunction (24), myocardial adipose deposition (25,26), pulmonary hypertension, impaired vasculature (27), abnormalities in the periphery, comorbidity-driven systemic inflammation (28). These factors are associated with HFpEF and contribute to the differences between patients with HFpEF and others (29). In the early stage of the disease, the myocardial mechanics' state can predict the evolution of different HF phenotypes (30). Earlier recognition of subtle abnormalities

in at-risk individuals made an earlier intervention of HFpEF patients possible, especially those with a history of CMI.

The reduced radial PEDSR and circumferential PEDSR of LV demonstrated the impaired early diastolic function of HFpEF-CMI patients, which was thought to be related to impaired active early relaxation and reduced compliance from increased ventricular stiffness (31). In addition, the diastolic function is an early hallmark of myocardial ischemia as early active relaxation is highly energy-dependent (32). The present study corroborated previous findings that LV longitudinal PLDSR was also significantly decreased in HFpEF patients (14). A higher RV longitudinal PLDSR in HFpEF-CMI group than in non-HF-CMI group was observed in current study. The patients with HFpEF-CMI were more likely to have a lower ratio

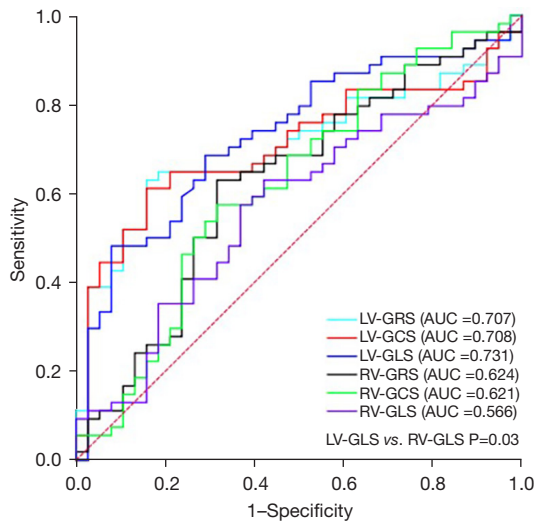


Figure 5 ROC curve analysis of CMR-TT derived LV and RV parameters for differentiating HFpEF-CMI from non-HF-CMI group. CMR, cardiac magnetic resonance; TT, tissue tracking; LV, left ventricular; RV, right ventricular; AUC, area under ROC curve; GRS, global radial strain; GCS, global circumferential strain; GLS, global longitudinal strain; ROC, receiver operating characteristic; HFpEF, heart failure with preserved ejection fraction; HF, heart failure; CMI, chronic myocardial infarction.

Table 5 Univariable association with HFpEF-CMI

Variables	OR (95% CI)	P
BMI ≥ 25 kg/m ²	3.73 (1.56–8.94)	0.003
MI volume $\geq 9.3\%$ LV	3.34 (1.40–7.95)	0.006
LV-GRS $\leq 24.4\%$	9.07 (3.23–25.45)	<0.001
LV-GCS $\geq -15.2\%$	10.37 (3.49–30.79)	<0.001
LV-GLS $\geq -11.5\%$	10.83 (2.97–39.52)	<0.001

HFpEF, heart failure with preserved ejection fraction; HF, heart failure; CMI, chronic myocardial infarction; OR, odds ratio; CI, confidence interval; BMI, body mass index; MI, myocardial infarction; LV, left ventricular; GRS, global radial strain; GCS, global circumferential strain; GLS, global longitudinal strain.

of PEDSR and PLDSR than non-HF-CMI. However, no difference that reaching statistical significance between the ratios was found in the results, which may be linked with sample size.

CMR was recommended for specialized diagnostic tests for patients with chronic HF to detect reversible/treatable causes of HF in conjunction with other non-invasive and invasive testing (2). As a feasible and reproducible

technique for assessing LV myocardial deformation, especially at the global level (33), CMR-TT is a validated non-invasive diagnostic tool for HFpEF patients (34). It provides multidimensional parameters for patients with HF. The incremental value of GCS, GLS, LVEF, and LGE in reflecting diastolic and systolic dysfunction in HFpEF was proved in many studies (20,35–38). Additionally, their combined prognostic value was assessed in a large-scale cohort of 539 patients (39). In the present study, the LV parameters significantly correlated with LVEF and NT-proBNP. NT-proBNP and BNP are essential metrics for the diagnosis of HF. Lower NT-proBNP levels in HFpEF relate more closely to muscle mass and are the most valuable prognostic factor (40–42). In summary, the correlations and respective unique roles of these values make them useful in future risk stratification of patients with HFpEF. Compared to a study targeting HFpEF with essential hypertension (HFpEF-HTN) patients, we got a relatively lower correlation coefficient between LVEF and LV strain parameters than their study (15). This difference may be caused by the LVEF derived from different examinations; they are from CMR, while ours are from TTE. We attempt to systematically measure the correlations between LV strain parameters and transmural, MI sizes. Nevertheless, we found that transmural was not statistically significantly correlated with LV strain parameters. The MI sizes has more reference value in evaluating the heart function than transmural but is still weakly correlated with the LV strain parameters.

Despite being widely used for subclassifying HF phenotypes, LVEF is not a sensitive marker of subtle damage in myocardial function (1). LV-GLS is increasingly thought to be a valuable prognostic parameter in patients with HFpEF, which appears to have a superior prognostic value to LVEF (43). In the present study, LV-GLS showed the highest specificity and the biggest AUC among the strain parameters. However, no significant difference was shown in the comparison of ROC curves of LV strain parameters. LV-GLS, LV-GCS, LV-GRS, and MI sizes were the independent contributors to the diagnosis of HFpEF-CMI in the multi-logistic analysis models. GLS derived from TTE is one of the minor criteria parameters of the HFA-PEFF diagnostic algorithm (10). CMR-TT derived LV strain parameters may become essential indices in a new diagnostic model or algorithm to assess cardiac dysfunction in all patients with HF. The combined multivariable models of clinical variables and CMR parameters had incremental diagnostic value. Prospective studies are needed to detect

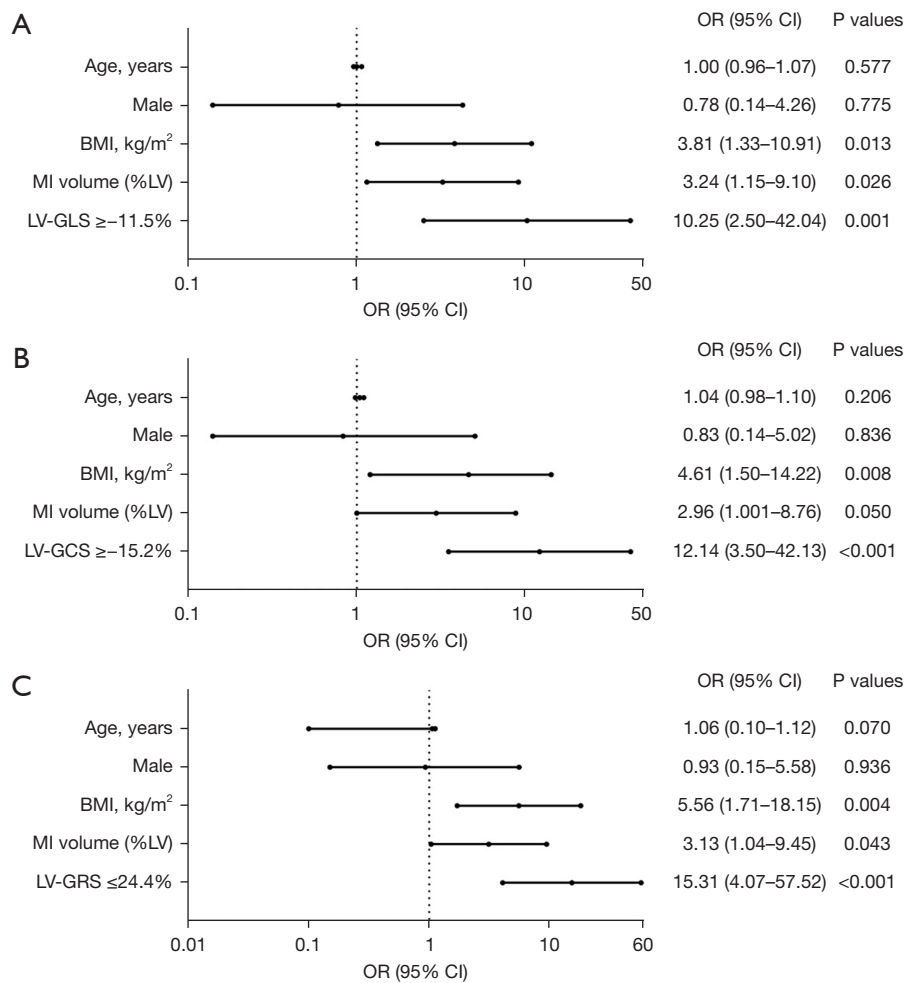


Figure 6 Diagnostic value of multiple regression model for HFpEF-CMI. (A) Model 1; (B) Model 2; (C) Model 3. Statistical significance was considered achieved at a P value <0.05. BMI, body mass index; MI, myocardial infarction; LV, left ventricular; OR, odds ratio; CI, confidence interval; GRS, global radial strain; GCS, global circumferential strain; GLS, global longitudinal strain; HFpEF, heart failure with preserved ejection fraction; HF, heart failure; CMI, chronic myocardial infarction.

Table 6 Intra- and interobserver reproducibility for strain parameters

Variables	Intraobserver		Interobserver	
	ICC	95% CI	ICC	95% CI
LV-GRS	0.942	0.860–0.977	0.976	0.872–0.982
LV-GCS	0.952	0.882–0.981	0.819	0.540–0.929
LV-GLS	0.953	0.886–0.981	0.985	0.956–0.994
RV-GRS	0.767	0.503–0.900	0.957	0.894–0.983
RV-GCS	0.863	0.689–0.943	0.759	0.382–0.905
RV-GLS	0.888	0.742–0.954	0.947	0.867–0.979

LV, left ventricular; RV, right ventricular; GRS, global radial strain; GCS, global circumferential strain; GLS, global longitudinal strain; ICC, intraclass correlation coefficient; CI, confidence interval.

models providing risk stratification, especially in patients with HFpEF.

In the present study, we included the CMI patients, which may introduce an overall selection bias. There is a high proportion of males (85%) in our experimental group, similar to a multicenter study performed by Gatzoulis *et al.* (44), in that 86.2% of preserved HF patients post-MI were men. IHD is an underlying pathogenic factor in HF, increasing the risk of HF 8-fold and with a population-attributable risk of 65% in men and 48% in women (45), and poorer prognosis due to IHD were experienced by men than women (46). Furthermore, we divided the HFpEF-CMI group into different subgroups according to gender, and there were no differences in both LV and RV strain values between males and females (Table S3).

Limitations

As an observational analysis with relatively small samples, the present study cannot provide more information on the prognostic value of CMR parameters. The causality between the causes of the change of strain values and preserved EF cannot be inferred. Further prospective clinical trials with larger sample sizes and sophisticated data are needed. In addition, HFpEF-CMI patients with a high proportion of males may not be the typical cohort for HFpEF. Therefore, our findings may not be generalizable to all patients with HFpEF but give evidence for further studies.

Conclusions

CMR-TT provides clinicians with useful additional imaging parameters to facilitate the assessment of CMI patients with HFpEF. LV strain parameters can detect early cardiac insufficiency in patients with HFpEF-CMI and have potential value for discriminating between HFpEF and non-HF patients post-CMI. Early detection and ongoing monitoring of CMI patients with HFpEF based on CMR-TT could be necessary.

Acknowledgments

Funding: This study was supported by the National Natural Science Foundation of China (Grant Nos. 81871435, 82071920 and 82171918). The funders had no role in the study design, data collection and analysis, decision to publish, or manuscript preparation.

Footnote

Reporting Checklist: The authors have completed the STARD reporting checklist. Available at <https://qims.amegroups.com/article/view/10.21037/qims-22-793/rc>

Conflicts of Interest: All authors have completed the ICMJE uniform disclosure form (available at <https://qims.amegroups.com/article/view/10.21037/qims-22-793/coif>). TL serves as an unpaid editorial board member of *Quantitative Imaging in Medicine and Surgery*. The authors have no conflicts of interest to declare.

Ethical Statement: The authors are accountable for all aspects of the work in ensuring that questions related to the accuracy or integrity of any part of the work are appropriately investigated and resolved. The study was conducted in accordance with the Declaration of Helsinki (as revised in 2013). This study was approved by the ethics committee of The First Hospital of China Medical University (reference No. KT2021213). All subjects provided written informed consent.

Open Access Statement: This is an Open Access article distributed in accordance with the Creative Commons Attribution-NonCommercial-NoDerivs 4.0 International License (CC BY-NC-ND 4.0), which permits the non-commercial replication and distribution of the article with the strict proviso that no changes or edits are made and the original work is properly cited (including links to both the formal publication through the relevant DOI and the license). See: <https://creativecommons.org/licenses/by-nc-nd/4.0/>.

References

1. Bozkurt B, Coats AJS, Tsutsui H, Abdelhamid CM, Adamopoulos S, Albert N, et al. Universal definition and classification of heart failure: a report of the Heart Failure Society of America, Heart Failure Association of the European Society of Cardiology, Japanese Heart Failure Society and Writing Committee of the Universal Definition of Heart Failure: Endorsed by the Canadian Heart Failure Society, Heart Failure Association of India, Cardiac Society of Australia and New Zealand, and Chinese Heart Failure Association. *Eur J Heart Fail* 2021;23:352-80.
2. McDonagh TA, Metra M, Adamo M, Gardner RS,

- Baumbach A, Böhm M, et al. 2021 ESC Guidelines for the diagnosis and treatment of acute and chronic heart failure. *Eur Heart J* 2021;42:3599-726.
3. Hiebert JB, Vacek J, Shah Z, Rahman F, Pierce JD. Use of speckle tracking to assess heart failure with preserved ejection fraction. *J Cardiol* 2019;74:397-402.
 4. Pothineni NV, Kattoor AJ, Kovelamudi S, Kenchaiah S. The Current Focus of Heart Failure Clinical Trials. *J Card Fail* 2018;24:321-9.
 5. Vedin O, Lam CSP, Koh AS, Benson L, Teng THK, Tay WT, Braun OÖ, Savarese G, Dahlström U, Lund LH. Significance of Ischemic Heart Disease in Patients With Heart Failure and Preserved, Midrange, and Reduced Ejection Fraction: A Nationwide Cohort Study. *Circ Heart Fail* 2017;10:e003875.
 6. Kanagala P, Cheng ASH, Singh A, McAdam J, Marsh AM, Arnold JR, Squire IB, Ng LL, McCann GP. Diagnostic and prognostic utility of cardiovascular magnetic resonance imaging in heart failure with preserved ejection fraction - implications for clinical trials. *J Cardiovasc Magn Reson* 2018;20:4.
 7. Marwick TH, Shah SJ, Thomas JD. Myocardial Strain in the Assessment of Patients With Heart Failure: A Review. *JAMA Cardiol* 2019;4:287-94.
 8. Huo H, Dai X, Li S, Zheng Y, Zhou J, Song Y, Liu S, Hou Y, Liu T. Diagnostic accuracy of cardiac magnetic resonance tissue tracking technology for differentiating between acute and chronic myocardial infarction. *Quant Imaging Med Surg* 2021;11:3070-81.
 9. Thygesen K, Alpert JS, Jaffe AS, Chaitman BR, Bax JJ, Morrow DA, White HD; . Fourth Universal Definition of Myocardial Infarction (2018). *Circulation* 2018;138:e618-51.
 10. Pieske B, Tschöpe C, de Boer RA, Fraser AG, Anker SD, Donal E, et al. How to diagnose heart failure with preserved ejection fraction: the HFA-PEFF diagnostic algorithm: a consensus recommendation from the Heart Failure Association (HFA) of the European Society of Cardiology (ESC). *Eur Heart J* 2019;40:3297-317.
 11. Ayton SL, Alfuhiel A, Gulsin GS, Parke KS, Wormleighton JV, Arnold JR, Moss AJ, Singh A, Xue H, Kellman P, Graham-Brown MPM, McCann GP. The Interfield Strength Agreement of Left Ventricular Strain Measurements at 1.5 T and 3 T Using Cardiac MRI Feature Tracking. *J Magn Reson Imaging* 2022. [Epub ahead of print]. doi: 10.1002/jmri.28328.
 12. Hanley JA, McNeil BJ. A method of comparing the areas under receiver operating characteristic curves derived from the same cases. *Radiology* 1983;148:839-43.
 13. Obuchowski NA, McClish DK. Sample size determination for diagnostic accuracy studies involving binormal ROC curve indices. *Stat Med* 1997;16:1529-42.
 14. Leng S, Tan RS, Zhao X, Allen JC, Koh AS, Zhong L. Fast long-axis strain: a simple, automatic approach for assessing left ventricular longitudinal function with cine cardiovascular magnetic resonance. *Eur Radiol* 2020;30:3672-83.
 15. He J, Sirajuddin A, Li S, Zhuang B, Xu J, Zhou D, Wu W, Sun X, Fan X, Ji K, Chen L, Zhao S, Arai AE, Lu M. Heart Failure With Preserved Ejection Fraction in Hypertension Patients: A Myocardial MR Strain Study. *J Magn Reson Imaging* 2021;53:527-39.
 16. Gerber Y, Weston SA, Berardi C, McNallan SM, Jiang R, Redfield MM, Roger VL. Contemporary trends in heart failure with reduced and preserved ejection fraction after myocardial infarction: a community study. *Am J Epidemiol* 2013;178:1272-80.
 17. Badar AA, Perez-Moreno AC, Hawkins NM, Jhund PS, Brunton AP, Anand IS, McKelvie RS, Komajda M, Zile MR, Carson PE, Gardner RS, Petrie MC, McMurray JJ. Clinical Characteristics and Outcomes of Patients With Coronary Artery Disease and Angina: Analysis of the Irbesartan in Patients With Heart Failure and Preserved Systolic Function Trial. *Circ Heart Fail* 2015;8:717-24.
 18. Hwang SJ, Melenovsky V, Borlaug BA. Implications of coronary artery disease in heart failure with preserved ejection fraction. *J Am Coll Cardiol* 2014;63:2817-27.
 19. Borlaug BA. The pathophysiology of heart failure with preserved ejection fraction. *Nat Rev Cardiol* 2014;11:507-15.
 20. Kraigher-Krainer E, Shah AM, Gupta DK, Santos A, Claggett B, Pieske B, Zile MR, Voors AA, Lefkowitz MP, Packer M, McMurray JJ, Solomon SD; . Impaired systolic function by strain imaging in heart failure with preserved ejection fraction. *J Am Coll Cardiol* 2014;63:447-56.
 21. Lüscher TF. Heart failure and left ventricular remodelling in HFrEF and HFpEF. *Eur Heart J* 2016;37:423-4.
 22. Garg P, Assadi H, Jones R, Chan WB, Metherall P, Thomas R, van der Geest R, Swift AJ, Al-Mohammad A. Left ventricular fibrosis and hypertrophy are associated with mortality in heart failure with preserved ejection fraction. *Sci Rep* 2021;11:617.
 23. Kanagala P, Cheng ASH, Singh A, Khan JN, Gulsin GS, Patel P, Gupta P, Arnold JR, Squire IB, Ng LL, McCann GP. Relationship Between Focal and Diffuse Fibrosis Assessed by CMR and Clinical Outcomes in Heart Failure

- With Preserved Ejection Fraction. *JACC Cardiovasc Imaging* 2019;12:2291-301.
24. Sanchis L, Gabrielli L, Andrea R, Falces C, Duchateau N, Perez-Villa F, Bijmens B, Sitges M. Left atrial dysfunction relates to symptom onset in patients with heart failure and preserved left ventricular ejection fraction. *Eur Heart J Cardiovasc Imaging* 2015;16:62-7.
 25. Pugliese NR, Paneni F, Mazzola M, De Biase N, Del Punta L, Gargani L, Mengozzi A, Viridis A, Nesti L, Taddei S, Flammer A, Borlaug BA, Ruschitzka F, Masi S. Impact of epicardial adipose tissue on cardiovascular haemodynamics, metabolic profile, and prognosis in heart failure. *Eur J Heart Fail* 2021;23:1858-71.
 26. Wu CK, Lee JK, Hsu JC, Su MM, Wu YF, Lin TT, Lan CW, Hwang JJ, Lin LY. Myocardial adipose deposition and the development of heart failure with preserved ejection fraction. *Eur J Heart Fail* 2020;22:445-54.
 27. Vancheri F, Longo G, Vancheri S, Henein M. Coronary Microvascular Dysfunction. *J Clin Med* 2020;9:2880.
 28. Schiattarella GG, Sequeira V, Ameri P. Distinctive patterns of inflammation across the heart failure syndrome. *Heart Fail Rev* 2021;26:1333-44.
 29. Quarta G, Gori M, Iorio A, D'Elia E, Moon JC, Iacovoni A, Burocchi S, Schelbert EB, Brambilla P, Sironi S, Caravita S, Parati G, Gavazzi A, Maisel AS, Butler J, Lam CSP, Senni M. Cardiac magnetic resonance in heart failure with preserved ejection fraction: myocyte, interstitium, microvascular, and metabolic abnormalities. *Eur J Heart Fail* 2020;22:1065-75.
 30. Bianco CM, Farjo PD, Ghaffar YA, Sengupta PP. Myocardial Mechanics in Patients With Normal LVEF and Diastolic Dysfunction. *JACC Cardiovasc Imaging* 2020;13:258-71.
 31. Rommel KP, von Roeder M, Latuscynski K, Oberueck C, Blazek S, Fengler K, Besler C, Sandri M, Lücke C, Gutberlet M, Linke A, Schuler G, Lurz P. Extracellular Volume Fraction for Characterization of Patients With Heart Failure and Preserved Ejection Fraction. *J Am Coll Cardiol* 2016;67:1815-25.
 32. Fischer K, Guensch DP, Jung B, King I, von Tengg-Kobligk H, Giannetti N, Eberle B, Friedrich MG. Insights Into Myocardial Oxygenation and Cardiovascular Magnetic Resonance Tissue Biomarkers in Heart Failure With Preserved Ejection Fraction. *Circ Heart Fail* 2022;15:e008903.
 33. Qu YY, Paul J, Li H, Ma GS, Buckert D, Rasche V. Left ventricular myocardial strain quantification with two- and three-dimensional cardiovascular magnetic resonance based tissue tracking. *Quant Imaging Med Surg* 2021;11:1421-36.
 34. Barison A, Aimo A, Todiere G, Grigoratos C, Aquaro GD, Emdin M. Cardiovascular magnetic resonance for the diagnosis and management of heart failure with preserved ejection fraction. *Heart Fail Rev* 2022;27:191-205.
 35. Ito H, Ishida M, Makino W, Goto Y, Ichikawa Y, Kitagawa K, Omori T, Dohi K, Ito M, Sakuma H. Cardiovascular magnetic resonance feature tracking for characterization of patients with heart failure with preserved ejection fraction: correlation of global longitudinal strain with invasive diastolic functional indices. *J Cardiovasc Magn Reson* 2020;22:42.
 36. van Woerden G, van Veldhuisen DJ, Gorter TM, Willems TP, van Empel VPM, Peters A, Pundziute G, Op den Akker JW, Rienstra M, Westenbrink BD. The clinical and prognostic value of late Gadolinium enhancement imaging in heart failure with mid-range and preserved ejection fraction. *Heart Vessels* 2022;37:273-81.
 37. He J, Yang W, Wu W, Li S, Yin G, Zhuang B, Xu J, Sun X, Zhou D, Wei B, Sirajuddin A, Teng Z, Zhao S, Kureshi F, Lu M. Early Diastolic Longitudinal Strain Rate at MRI and Outcomes in Heart Failure with Preserved Ejection Fraction. *Radiology* 2021;301:582-92.
 38. Kammerlander AA, Kraiger JA, Nitsche C, Donà C, Duca F, Zotter-Tufaro C, Binder C, Aschauer S, Loewe C, Hengstenberg C, Bonderman D, Mascherbauer J. Global Longitudinal Strain by CMR Feature Tracking Is Associated With Outcome in HFPEF. *JACC Cardiovasc Imaging* 2019;12:1585-7.
 39. Mordi I, Bezerra H, Carrick D, Tzemos N. The Combined Incremental Prognostic Value of LVEF, Late Gadolinium Enhancement, and Global Circumferential Strain Assessed by CMR. *JACC Cardiovasc Imaging* 2015;8:540-9.
 40. Selvaraj S, Kim J, Ansari BA, Zhao L, Cvijic ME, Fronheiser M, et al. Body Composition, Natriuretic Peptides, and Adverse Outcomes in Heart Failure With Preserved and Reduced Ejection Fraction. *JACC Cardiovasc Imaging* 2021;14:203-15.
 41. Kasahara S, Sakata Y, Nochioka K, Yamauchi T, Onose T, Tsuji K, Abe R, Oikawa T, Sato M, Aoyanagi H, Miura M, Shiroto T, Takahashi J, Miyata S, Shimokawa H; . Comparable prognostic impact of BNP levels among HFpEF, Borderline HFpEF and HFrEF: a report from the CHART-2 Study. *Heart Vessels* 2018;33:997-1007.
 42. Salah K, Stienen S, Pinto YM, Eurlings LW, Metra M, Bayes-Genis A, Verdiani V, Tijssen JGP, Kok WE.

- Prognosis and NT-proBNP in heart failure patients with preserved versus reduced ejection fraction. *Heart* 2019;105:1182-9.
43. Shah AM, Claggett B, Sweitzer NK, Shah SJ, Anand IS, Liu L, Pitt B, Pfeffer MA, Solomon SD. Prognostic Importance of Impaired Systolic Function in Heart Failure With Preserved Ejection Fraction and the Impact of Spironolactone. *Circulation* 2015;132:402-14.
44. Gatzoulis KA, Tsiachris D, Arsenos P, Antoniou CK, Dilaveris P, Sideris S, et al. Arrhythmic risk stratification in post-myocardial infarction patients with preserved ejection fraction: the PRESERVE EF study. *Eur Heart J* 2019;40:2940-9.
45. Lund LH, Mancini D. Heart failure in women. *Med Clin North Am* 2004;88:1321-45, xii.
46. Roth GA, Mensah GA, Johnson CO, Addolorato G, Ammirati E, Baddour LM, et al. Global Burden of Cardiovascular Diseases and Risk Factors, 1990-2019: Update From the GBD 2019 Study. *J Am Coll Cardiol* 2020;76:2982-3021.

Cite this article as: Li H, Zheng Y, Peng X, Liu H, Li Y, Tian Z, Hou Y, Jin S, Huo H, Liu T. Heart failure with preserved ejection fraction in post myocardial infarction patients: a myocardial magnetic resonance (MR) tissue tracking study. *Quant Imaging Med Surg* 2023;13(3):1723-1739. doi: 10.21037/qims-22-793

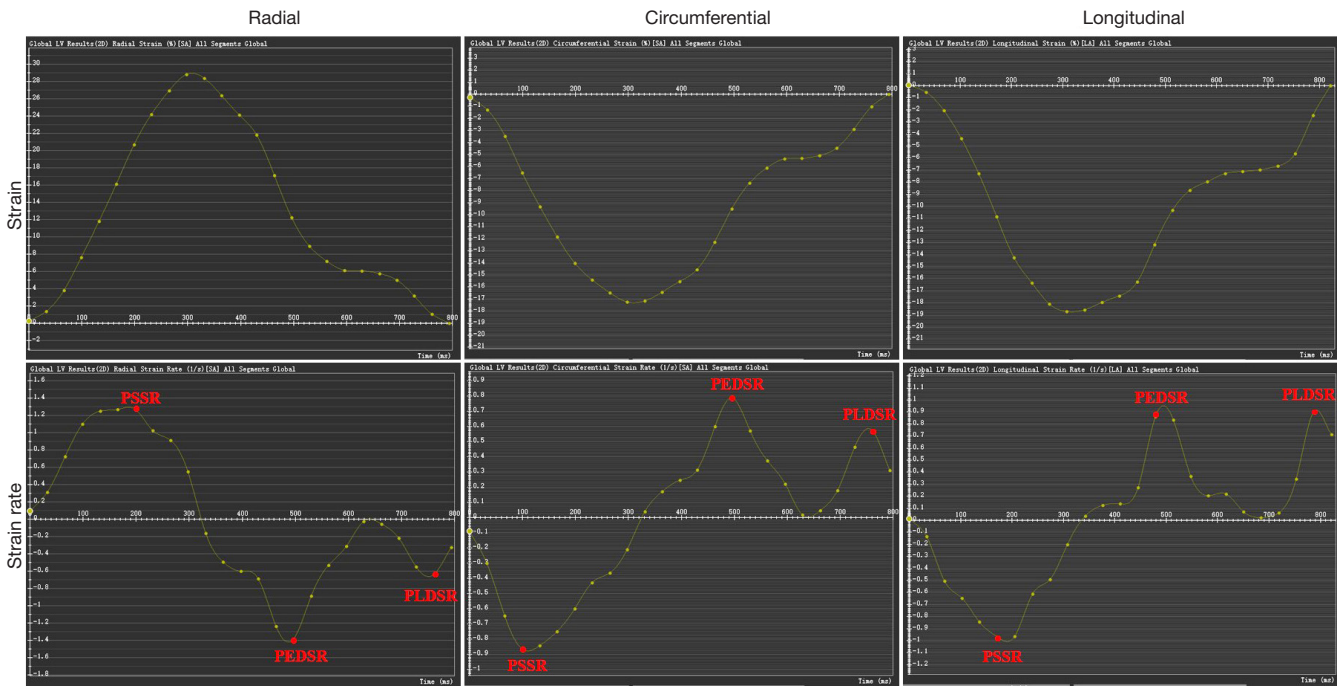


Figure S1 Representative example of image analysis for a single participant with LV-strain and strain rate graphs in the three directions. LV, left ventricular; 2D, two-dimensional; SA, short-axis; LA, long-axis; PSSR, peak systolic strain rate; PEDSR, peak early diastolic strain rate; PLDSR, peak late diastolic strain rate.

Table S1 Comparison of ROC curves of strain parameters for diagnosis of HFpEF-CMI

Variables	AUC (95% CI)	Z statistic	P
LV-GRS	0.707 (0.603–0.797)	–	–
LV-GCS	0.708 (0.604–0.798)	vs. LV-GRS: 0.049	vs. LV-GRS: 0.961
LV-GLS	0.731 (0.628–0.818)	vs. LV-GRS: 0.049 vs. LV-GCS: 0.475	vs. LV-GRS: 0.627 vs. LV-GCS: 0.634
RV-GRS	0.624 (0.517–0.723)	vs. LV-GRS: 1.172 vs. LV-GCS: 1.188 vs. LV-GLS: 1.442	vs. LV-GRS: 0.241 vs. LV-GCS: 0.234 vs. LV-GLS: 0.149
RV-GCS	0.621 (0.514–0.720)	vs. LV-GRS: 1.206 vs. LV-GCS: 1.219 vs. LV-GLS: 1.498	vs. LV-GRS: 0.228 vs. LV-GCS: 0.222 vs. LV-GLS: 0.134
RV-GLS	0.566 (0.458–0.669)	vs. LV-GRS: 1.852 vs. LV-GCS: 1.855 vs. LV-GLS: 2.149	vs. LV-GRS: 0.064 vs. LV-GCS: 0.064 vs. LV-GLS: 0.032

Statistical significance was considered achieved at a P value <0.05. ROC, receiver operating characteristic; HFpEF, heart failure with preserved ejection fraction; HF, heart failure; CMI, chronic myocardial infarction; AUC, area under the ROC curve; CI, confidence interval; LV, left ventricular; RV, right ventricular; GRS, global radial strain; GCS, global circumferential strain; GLS, global longitudinal strain.

Table S2 The reclassification table between different models using the Model 1 as reference model (the cut-off probability for high risk was set as 0.73)

Model 1: LV-GLS	Model 2: LV-GCS					Model 3: LV-GRS				
	Low risk	High risk	% Reclassified	Category NRI (95% CI)	P value	Low risk	High risk	% Reclassified	Category NRI (95% CI)	P value
HFpEF-CMI				Model 2 vs. Model 1: 0.011 (-0.134, 0.156)	0.88				Model 3 vs. Model 1: -0.008 (-0.148, 0.132)	0.91
Low risk	17	6	26			18	5	22		
High risk	4	27	13			4	27	13		
Non-HF-CMI										
Low risk	35	2	5			35	2	5		
High risk	1	0	100			1	0	100		

LV, left ventricular; CI, confidence interval; GRS, global radial strain; GCS, global circumferential strain; GLS, global longitudinal strain; HFpEF, heart failure with preserved ejection fraction; HF, heart failure; CMI, chronic myocardial infarction; NRI, net reclassification improvement.

Table S3 Comparison of the strains of different gender in the HFpEF-CMI group

Variables	Male (n=46)	Female (n=8)	P
LV-GRS, %	21.98±8.90	26.67±9.34	0.178
LV-GCS, %	-13.86±4.11	-16.00±3.88	0.178
LV-GLS, %	-11.92±3.22	-12.64±4.26	0.581
RV-GRS, %	27.85 (18.59–32.07)	24.92 (23.73–29.02)	0.990
RV-GCS, %	-13.91±3.96	-14.90±2.96	0.504
RV-GLS, %	-22.43 (-24.58 to -19.04)	-25.07 (-27.06 to -15.01)	0.306

Values are mean ± standard deviation or median (interquartile range). Statistical significance was considered achieved at a P value <0.05. HFpEF, heart failure with preserved ejection fraction; HF, heart failure; CMI, chronic myocardial infarction; LV, left ventricular; RV, right ventricular; GRS, global radial strain; GCS, global circumferential strain; GLS, global longitudinal strain.